6-2020

THE DEVELOPMENT OF AN H1 EMBRYONIC STEM CELL LINE TO STUDY THE ROLE OF THE ONCOGENES LMO1 AND MYCN IN HUMAN NEUROBLASTOMA FORMATION

Vincent Quiroz

THE DEVELOPMENT OF AN H1 EMBRYONIC STEM CELL LINE TO STUDY THE ROLE OF THE ONCOGENES LMO1 AND MYCN IN HUMAN NEUROBLASTOMA FORMATION

A Thesis

Presented to the

Faculty of

California State University,

San Bernardino

In Partial Fulfillment

of the Requirements for the Degree

Master of Science

in

Biology

by

Vincent Quiroz

June 2020

THE DEVELOPMENT OF AN H1 EMBRYONIC STEM CELL LINE TO STUDY THE ROLE OF THE ONCOGENES LMO1 AND MYCN IN HUMAN NEUROBLASTOMA FORMATION

A Thesis

Presented to the

Faculty of

California State University,

San Bernardino

---

by

Vincent Quiroz

June 2020

Approved by:

Nicole Bournias-Vardiabasis, Committee Chair, Biology

Martín Garcia-Castro, Committee Member

Michael Chao, Committee Member

ABSTRACT

Neuroblastoma (NB) is an extracranial tumor that affects the nervous system and accounts for approximately 650 – 800 cases diagnosed per year in children under the age of 5 (www.cancer.org/cancer/neuroblastoma/about/key-statistics.html). NB occurs at a relatively rare rate of 10.2 per million children under 15 years old but accounts for 12-15% of pediatric cancer death because patients with high-risk NB (HRNB) have 5-year survival rates between 40-50%(Brodeur, 2003; Park et al. 2010). Developmental biology research has recognized neural crest cells (NCC) as the progenitor cells of NB, as tumors form in the trunk NC derived sympathetic nervous system (Dupin, 2013; Simões-Costa et al., 2015). Genome-wide association studies (GWAS) of these tumors reveal several chromosomal aberrations and genes related to the development of NB (Pugh et al., 2013; Seeger et al., 1985). Unfortunately, the heterogeneity of the disease has revealed a low mutation frequency in suspected oncogenes, along with an assortment of chromosomal gains and losses, resulting in a variety of mechanisms of NB formation. These structural features demonstrate the complexity of NB tumorigenesis and the unlikeliness of developing a single target treatment (Matthay, K et al., 2012). Amongst all the predictors recognized in NB formation, amplification of the MYCN gene occurs in 20% of tumors and serves as the most significant prognosticator of poor outcomes in HRNB patients (Brodeur, 1984). These insights have resulted in NCC experiments in mice, zebrafish, and primary cell models to study NB development under the

overexpression of MYCN and other oncogenes such as ALK and LMO1(Weiss et al.,1997; Zhu et al., 2012; Olsen et al., 2017). While these models have elucidated the association of MYCN and LMO1 overexpression in NCC to NB formation, they lack a direct descriptive model of NB formation in human NCC.

Building off the current understanding of genes synergistically driving neuroblastoma, I utilized H1 human embryonic stem cells (hESC) to create a cell line inducible for LMO1 and MYCN. Through genetic engineering, and subcloning, I created two constructs: a plasmid containing the MYCN gene under the regulation of the Tetracycline On (TET-ON) system and the LMO1 construct under the regulation of TET-ON. I sequenced the constructs, analyzed their genetic composition, and found the TET-ON LMO1 suitable for integration into the H1 hESC. After nucleofection and genetic screening, the data suggest the production of a mixed population of H1 hESC containing a subset of cells that appear to have integrated the TET-ON LMO1 into the AAVS1 locus at chromosome 19. Further attempts are required for the complete development of the H1 hESC TET- 3G LMO1 plus MYCN inducible cell line.

ACKNOWLEDGEMENTS

I want to thank Dr. Nicole Bournias-Vardiabasis, who permitted me the opportunity to be a part of the CIRM-Bridges cohort of 2019. Under her mentorship, I was able to explore my interests in epidemiology and public health, which shaped my decision to apply to public health Ph.D. programs. I want to thank Dr. Chao, for his willingness to partake in my committee and support my journey through the master program during this unprecedented period in history. I want to thank Dr. Martín Garcia-Castro for welcoming me into his laboratory and making me feel like a member of his team. The skills and critical thinking that I gained provide me a toolset that I will carry on in my career as a public health researcher. I would also like to extend my appreciation to Dr. Maneeshi Prasad and Dr. Rebekah Charney. The post-doctoral mentors that patiently and thoroughly trained me in molecular biology, genetic engineering, and cell culturing techniques crucial for my project. I want to thank Jonathan Cohen, my platoon commander from 2nd battalion 6th Marines, who has remained in contact for the last ten years and has supported my success outside of the Marine Corps.

TABLE OF CONTENTS

LIST OF TABLES

LIST OF FIGURES

CHAPTER ONE

NEURAL CREST CELL DEVELOPMENT AND ROLE IN NEUROBLASTOMA

Overview of Neural Crest Cells

Neural crest cells (NCC) are a population of multipotent progenitor cells that are unique to vertebrates that emerge early in development and migrate extensively to form a multitude of derivatives (Prasad et al., 2019). NCC differentiates into a variety of cell lineages, such as the sensory neurons and glia of the sympathetic and parasympathetic nervous system, hormone-producing cells of the adrenal gland, pigment-producing cells, and the connective and structural components of the craniofacial region (Simões-Costa, M., & Bronner, M. E. 2015). The migratory nature of NCC and their differentiation to a wide variety of cell types is accomplished through complex spatial-temporal intracellular and intercellular singling. Defects in NCC that produce birth defects are classified as neurocristopathies and are responsible for various diseases, including cleft lip/palate, Hirschsprung, Waardenburg syndromes, and cancers such as melanoma and neuroblastoma (Guillermo et al., 2018). Therefore, to understand the progression of neurocristopathy, researchers investigate the early development, genetic aberrations, signaling pathways, and cellular environment that influences improper NCC differentiation.

Neural Crest Development

Neural crest cells are a derivate of the ectoderm and develop during neurulation when the neural plate invaginates to form the neural tube. Research conducted in chicken and amphibian embryos has demonstrated that neural crest induction occurs in a two-step process. The first step involves WNT and FGF signaling, which promotes the formation of the neural plate border tissue, which flanks the neural plate and separates the neural and nonneural ectoderm. The second step of the induction process involves Wnt, BMP, and Notch pathways that are responsible for activating and maintaining neural crest cell specificity. While the signals responsible for the formation of neural crest cells are well characterized. There is much debate on how and what tissues interact in neural crest cell formation.

Neural crest cells develop along most of the dorsal axis of the neural tube and exhibit different migration patterns according to the signals received by the neural crest cells (Prasad et al., 2019). The NC has four distinct anatomical regions on the neural tube characterized by the derivatives they produce: cranial NC, cardiac NC, trunk NC, vagal/sacral NC. The cranial NC migrates to the pharyngeal arches and forms the craniofacial skeleton, parasympathetic and sensory ganglia, and endocrine and pigment cells (Gilbert, 2000). The cardiac NC is a subregion of the cranial NC, which develops into the neurons, cartilage, and connective tissues of the pharyngeal arches and the muscular-connective tissue of arteries (Gilbert, 2000; Huber. 2015). The trunk NC which forms the

dorsal root ganglia, the sympathetic ganglia, and melanocytes. The vagal/sacral NC form the parasympathetic ganglia of the gut, and these cell types are dispersed along the neural tube.

Trunk Neural Crest Derivatives and Neuroblastoma Formation

NB tumors are localized to the sympathetic nervous system, particularly the adrenal medulla has isolated the trunk NC as the population of cells involved in tumor formation. The trunk NC has two avenues of migration: the dorsolateral and the ventrolateral pathway. The dorsolateral pathway produces skin melanocytes, while the ventrolateral pathway produces the dorsal root ganglia, sympathetic ganglia, adrenal medulla, and aortic nerve clusters (Gilbert, 2000). It is the sympathetic ganglia and specifically the adrenal medulla, that is associated with the NB tumor formation. NB tumors are generally localized to one of the adrenal glands, but there is a small subset of NB patients that present bilateral tumors in both adrenal glands, suggesting NB tumorigenesis before the migration of the NC (Pagès et al., 2009). The migratory pattern of NCC, the location of tumors in the sympathetic chain, along with single and bilateral adrenal glands, provides evidence that NB is a derivative of the trunk NC.

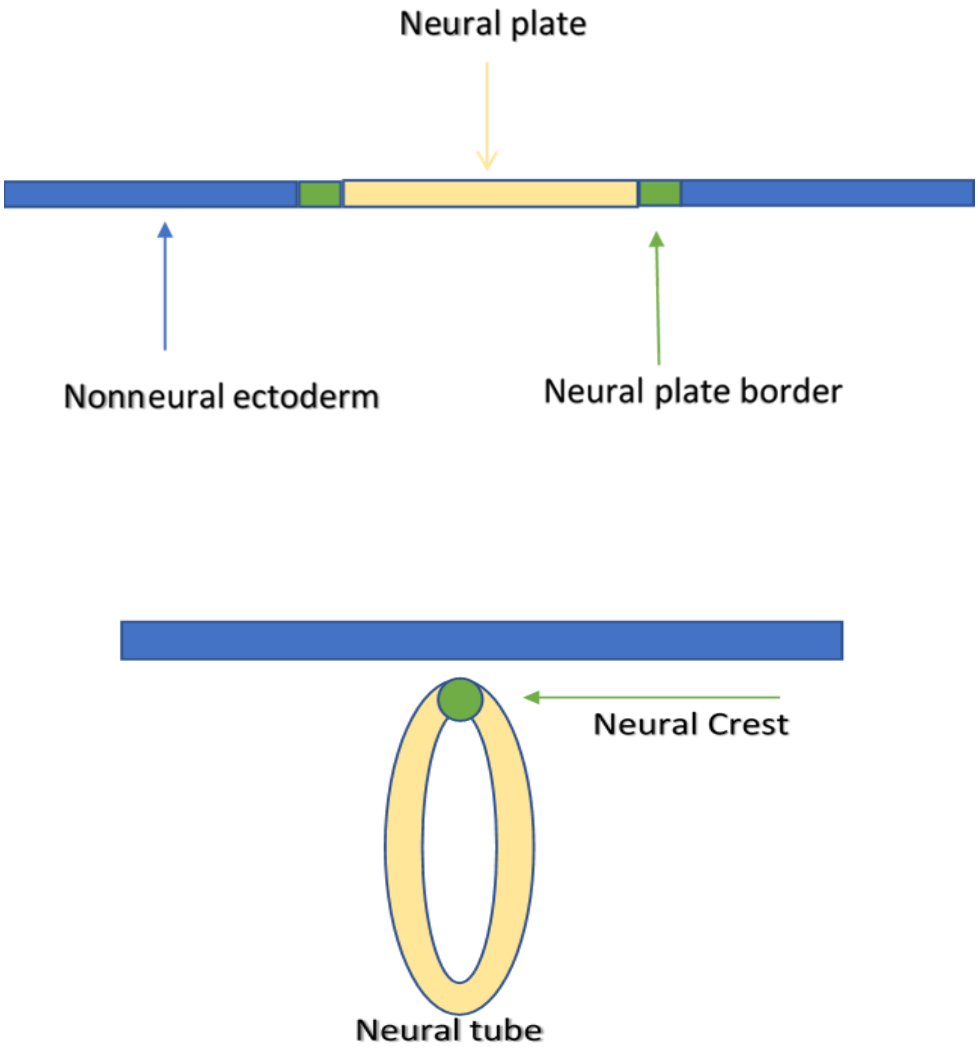

Figure 1. Neural Tube Formation.
Representation of the Ectoderm, Neural plate borders, and the Neural plate before the formation of the neural tube. The bottom portion of the diagram depicts the neural tube, neural crest, and ectoderm, which developed after the invagination of the neural plate and neural plate borders.

CHAPTER TWO

THE GENETICS AND MODELS OF NEUROBLASTOMA

Neuroblastoma Overview

The development of a cell line project that can model NB involves understanding the molecular and genetic features of the disease. This task required investigation into the clinical data of high-risk neuroblastoma patients and the emerging genome-wide association studies exploring the genomic and genetic structures involved in cancer. Genomic analysis of HRNB tumors has revealed the chromosomal aberrations and the genetic interactions that correspond to clinically favorable or unfavorable outcomes in patients (Cheung, N. K., & Dyer, M. A. 2013). There are two basic patterns of genomic modifications that impact NB prognosis. The first being whole chromosomal gain, which can produce a positive outcome in NB patients. The second involves segmental chromosomal losses, gains, or a combination of both, which results in MYCN amplification, loss of tumor suppressor function, or increased expression of other oncogenes. The genomic survey of tumors has revealed there is no single genetic mutation that corresponds with HRNB and reduced survival rates (Pugh TJ). This reality required the Garcia-Castro laboratory to develop a model that could generate neuroblastoma from the neural crest model.

Clinically Observed Chromosomal Aberrations in Neuroblastoma

Deletions in chromosome 1p36 occur in approximately 70% of tumors associated with an elevated risk of recurrence in patients (Kim, S. et al., 2006). The suspected cause of tumor formation is the loss of CHD5, a tumor suppressor gene that regulates the proliferation of cells in the nervous system (Colon, N. C., & Chung, D. H., 2011). The whole chromosomal gain of chromosome 17 tends to lead to a favorable outcome, but the somatic gain of chromosome 17q manifests in over 50% of Neuroblastomas cases correlated with poor survival outcomes (Van Roy et al., 2009). Chromosome 17q contains survivin/BIRC5 (an anti-apoptotic protein) and nm23/NME1 (nucleoside diphosphate kinases), which paired with MYCN overexpression lead to tumor growth and proliferation. Another recurrent chromosomal aberration that presents a different mechanism of NB formation is the somatic loss of chromosome 3q and 11q, which produces NB without MYCN overexpression (Van Roy et al., 2009). Chromosomal aberrations are indicative of failures of regulatory factors that result from a multifaceted loss of apoptotic genes and the gain of proto-oncogenes (Cheung, N. K., & Dyer, M. A., 2013. These aberrations have become clinically recognized as a predictor of risk in patients with NB.

Genes and Modes of Neuroblastoma Inheritance

MYCN belongs to the MYC family of oncogenes, whose deregulation appears in a variety of cancers and perhaps are involved in all human tumor formation (Dang, 2012). MYCN is located on chromosome 2p24.3 and produces the protein N-MYC which is necessary for the proliferation of progenitor cells during the development of the central nervous system (Knoepfler et al., 2002). MYCN expression is observable in the early neural crest cells, and in typical development, expression decreases as neuroblasts differentiate into their terminal cell type (Huang, M., & Weiss, W. A., 2013). Overexpression of MYCN appears in many cancers of the nervous system as well as nonneuronal tumors such as prostate cancers, but MYCN is most notably associated with high-risk neuroblastoma and poor prognosis in patients (Beltran et al., 2011; Seeger et al., 1985). In approximately 20% of NB tumors, the MYCN gene is amplified, presenting between 4 to 10 chromosomal copies (Modak, S., & Cheung, N. K., 2010). Despite the known oncogenic nature of MYCN in NB, its role as a critical transcription factor for development makes it an undesirable target for suppression (Kushner B. H. 2004). This reality has motivated researchers to identify the down streams pathway of N-MYC or synergistic genes that promote NB as possible therapeutic targets.

Familial NB is inherited in an autosomal dominant manner with incomplete penetrance that accounts for approximately 1-2% of all cases of NB (Colon, N. C., & Chung, D. H., 2011). Familial NB patients are generally diagnosed earlier

than sporadic cases and present many primary tumors and other clinical hallmarks associated with NB (Smith, V., & Foster, J. 2018). The inheritance pattern is described in the late 1960s due to cases where several siblings in a family would develop NB tumors in the sympathetic nervous system (Knudson, A. G., Jr, & Strong, L. C., 1972). In the mid to late 2000s, the genes PHOX2B and ALK were identified for the role they played in the familial inheritance pattern (Trochet et al., 2004; Janoueix-Lerosey et al., 2008). PHOX2B is a gene that encodes for a paired homeodomain transcription factor that regulates cell cycle, neuronal differentiation, and account for approximately 6-10% of familial cases (Mossé et al., 2004). ALK (anaplastic lymphoma kinase) is a gene that encodes a tyrosine kinase receptor that plays a role in neuronal differentiation, proliferation, survival (Mossé et al., 2008). Genome sequencing has identified several mutations in the ALK gene, which are the most aggressive type of familial NB, causing mutation resulting in the majority of primary neuroblastoma (Schulte et al., 2013). Familial NB, while well-characterized, remains the rarest form of NB, and much attention has is focused on the Sporadic formation of NB.

Sporadic NB is the most typical manner that tumors develop in the sympathetic chain, which results from somatic mutations that are not inherited. The most common mutation observed in sporadic NB is the gain of the MYCN gene copies, which express a high level of N-MYC protein. Genome-wide association studies (GWAS) have identified nine other genes involved in the pathogenesis of sporadic NB with BARD1, CASC15/14, LMO1, LIN28B, and

HACE1 observed in high-risk tumors (Bosse, K. R., & Maris, J. M., 2016). The LIM-domain-only (LMO1) gene, located at 11p15 is implicated across several epidemiological studies as an NB oncogene in human tumors (Matthews, J. M., Lester, K., Joseph, S., & Curtis, D. J., 2013). The somatic gain of 11p results in elevated levels of LMO1 expression, which is detected in tumors that have metastasized (Bach, 2000). Experiments demonstrate reducing LMO1 expression with short hairpin RNA lowered the growth of NB tumors while increasing LMO1 promotes tumor formation (Wang K, Diskin SJ, Zhang H, et al. 2011). The implications of LMO1 expression in HRNB has persuaded researchers to develop a model to study its role in NB formation.

Current Models of Neuroblastoma Research

Clinically the overexpression of MYCN has shown an association with neuroblastoma in several retroactive studies. However, the demonstration of MYCN expression initiating NB formation was absent in the literature (Olsen et al., 2017). Researchers established transgenic mice, zebrafish, and primary cell models to observe if MYCN overexpression was sufficient to drive NB. The goal of MYCN overexpression in a model organism is to promote tumor growth in the sympathetic nervous system, particularly the adrenal medulla, to resemble human neuroblastoma and identify a possible mechanism of tumorigenesis.

One of the first models that demonstrated MYCN's role in NB formation was a transgenic mouse model that overexpressed human MYCN in migrating

NCC. (Weiss et al. 1997). This novel murine model utilized a rat tyrosine hydroxylase promoter, and while NB tumors formed, the model was crude as MYCN expression was not robust, and strain background affected the level of tumor development (Althoff et al. 2015). The transgenic mouse line LSL-MYCN; Dbh-iCre (Cre-conditional induction of MYCN in dopamine- β- hydroxylase-expressing cells) was created to overcome the lack of robust expression in all mice strain (Althoff et al. 2015). The transgenic mice developed tumors with an incidence of >75% regardless of the original strain. Specific expression of MYCN in the neural crest produced abdominal tumors, which had a histology and expression markers typical of human NB (Rickman et al. 2018). Genomic analysis of the tumors revealed chromosomal aberrations syntenic to human NB, specifically the murine partial gain of 11q, which is homologous to human chromosome 17q – A frequent segmental chromosomal gain in human NB (Vandesompele et al. 2005). The LSL-MYCN; Dbh-iCre mouse established a model of advancing neuroblastoma from MYCN overexpression. This experiment makes it plausible that similar results may be repeated in human NCC with MYCN overexpression.

GWAS of HRNB tumors observed an association with LMO1 concentration and the development of aggressive cancers in human patients (Wang K, Diskin SJ, Zhang H, et al. 2011). Researchers interested in the influence of the oncogenes LMO1 and MYCN on NB created transgenic zebrafish lines expressing human LMO1 (dβh LMO1,) MYCN(dβh MYCN), and

LMO1 with MYCN (dβh MYCN; LMO1) under a dopamine-β-hydroxylase(dβh) gene promoter (Zhu et al., 2017). The authors did not observe tumor formations in the cell line dβh LMO1 when LMO1 expression was high in the absence of high MCYN expression. The transgenic zebrafish that overexpressed MYCN only accrued 20-30% tumor formation within its population, while the double mutant dβh MYCN; LMO1 contained 80% tumor formation in its population of zebrafish. The experiment showed that high expression of LMO1 when in collaboration with high levels of MYCN expression leads to the accelerated onset of NB in vivo (Zhu et al., 2017). The finding in the zebrafish model demonstrates that LMO1 interacts synergistically with MYCN to drive HRNB (Wang et al., 2011). This model begs the question if LMO1 and MYCN interact similarly in human NB development.

Animals models have proved a useful tool in studying many diseases, though there are generally expensive, time-consuming, and lack scalability. Researchers utilize primary cell models to address some of the animal model limitations and gain the ability to observe the cellular properties of tissues in vitro. In the case of NB, animal models have shown tumor formation in the overexpression of MYCN and LMO1 in NCC. The primary NCC model was developed to study the early stages of NB oncogenesis, assess the oncogenic drivers, and characterized NB metastasis. The primary NCC were isolated from the trunk neural tube of heterozygous p53+/- mice (embryonic day 9.5), and the signal markers Sox10 and p75 verified the cells were uncommitted NCC (Olsen

et al. 2019; Kim, J. et al. 2003). The extracted cells were transduced with N-Myc-IRES-GFP retrovirus and reintroduced into nude and C57BI/6 mice (Kawauchi et al., 2012). There was 100% tumor penetrance in the eight nude mice and six C57BI/6. NCC tumors were analyzed for chromosomal aberrations, which revealed chromosomal gains and losses analogous to human MYCN amplified NB (Olsen et al. 2019). The modification of murine neural crest cells to form neuroblastoma by the overexpression of MYCN provided the evidence we could translate this research into human neural crest cells.

CHAPTER THREE

THE CREATION OF THE CELL LINE

A Human Neuroblastoma Model

The overexpression of LMO1 and MYCN in clinically observed human tumors and their direct involvement in driving NB in animal and cell models makes these two genes rather appropriate to study in a human system. A popular human model for studying human diseases is the use of human stem cells, either induced pluripotent stem (IPSC) or embryonic stem cells (ESCs). IPSCs are reprogramed from adult cells to become pluripotent. The adult cell is obtained from an individual that has a disease and is studied to develop a patient-specific treatment. In the case of NB, there are examples of IPSC lines, but these cell lines carry the genetic mutations of the patient, which is advantageous in therapy design, but not for developmental research (Marin et al. 2019). The advantage of ESCs is that they permit researchers to modify the human genome with the genes they wish to study and differentiate them into the cells or tissue of their research model. Our laboratory is primarily concerned with the development of neuroblastoma from neural crest cells, so ESC is the model that permits us to examine the role of LMO1 and MYCN in the human development of NCC.

H1 Cell Line Design

The construction of the cell line required the development of plasmid constructs that integrated LMO1 and MYCN into the H1 ESC genome and permitted controlled expression. The TET-3G plasmid (AAVS1 Puro Tet3G 3xFLAG Twin Strep. Addgene catalog # 92099) was selected because of the homologous arms in the plasmid specific to the AAVS1 locus and the TET-ON inducible system. The homologous arm right is 837 bases and the homologous arm left is 804 bases these sequences are specific to the AAVS1 locus at human chromosome 19. The AAVS1 locus is popularly labeled the “safe harbor” as it allows reliable integration of genes by homology driven repair under CRISPR Cas9 modification (Sadelain, M., Papapetrou, E. P., & Bushman, F. D., 2011). This technique in the past been shown to be highly efficient in modifying hESC genomes, and experiments report low off-target alteration (Castaño et al., 2017). TET-ON is a gene regulatory system that allows for the reliable and tight expression of a gene in the presence of the molecule doxycycline – a small molecule demonstrated not to produce cytotoxic effects or unwanted differentiation of cells in gene therapy application (Das, A. T., Tenenbaum, L., & Berkhout, B. 2016)

Isolation of Human LMO1 and MYCN Genes

The LMO1 protein-encoding gene was isolated from 3-day old neural crest cells cDNA to design the TET-3G LMO1 construct for integration into the AAVS1 locus.

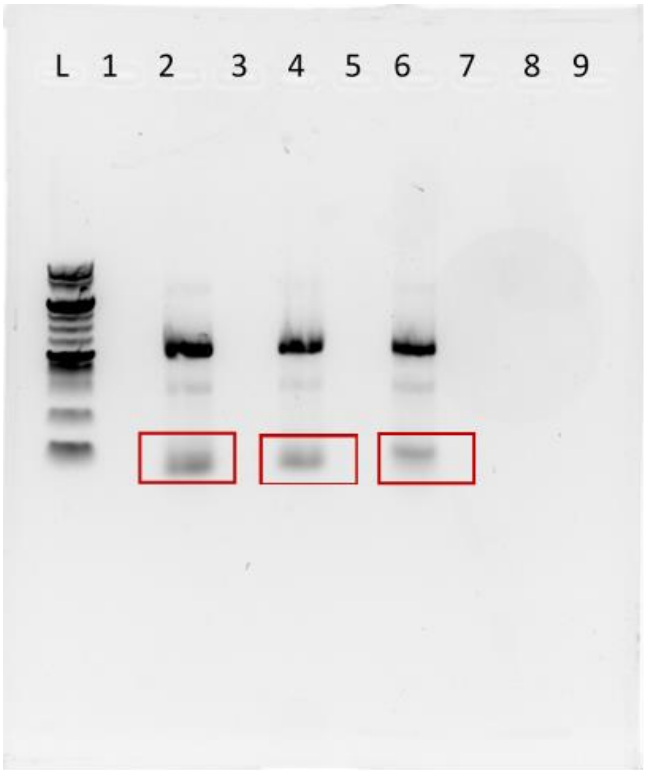

Figure 2. Agarose Gel of the LMO1 Gene.
Isolated from Day 3 neural crest cell cDNA library maintained by the Garcia-Castro laboratory. The products are 463 base pairs in length and are in lanes 2, 4, and 6.

The MYCN cDNA was isolated from the pCDNA3-HA-human W- MYCN (MYCN donor) plasmid to construct the TET-3G MYCN plasmid for integration to the AAVS1 locus.

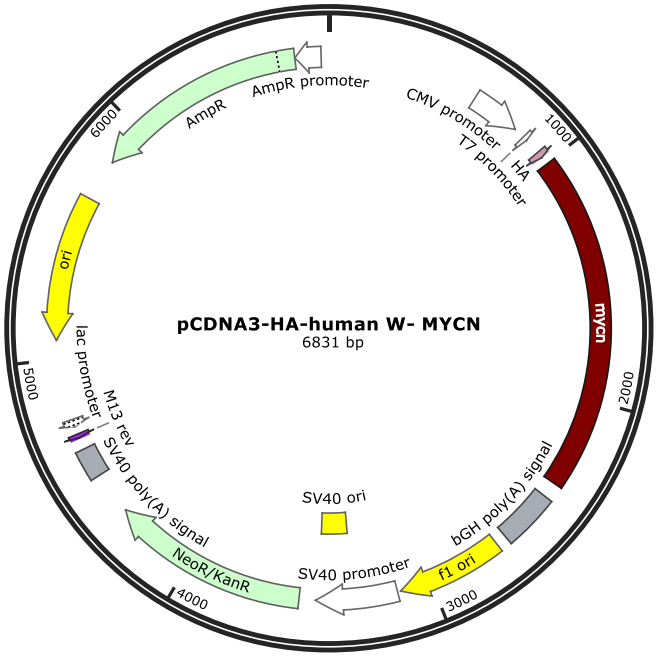

Figure 3. MYCN Donor Plasmid.
The pCDNA3-HA human plasmid contained MYCN protein-coding sequence which was purchased from addgene to isolate the MYCN DNA sequence.

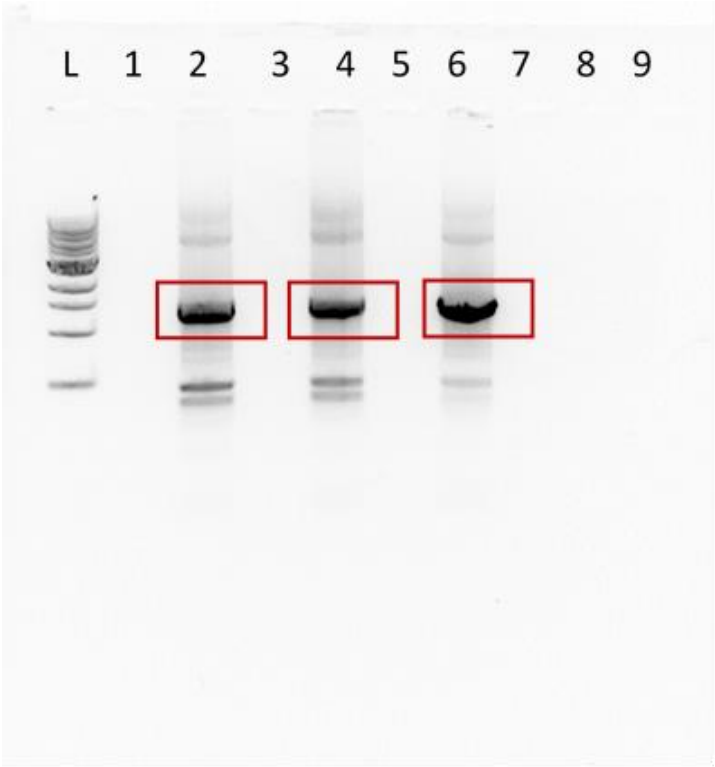

Figure 4. Agarose Gel of the MYCN Gene.
Isolated from the MYCN donor plasmid. The products are 1392 bases and visible in lanes 2, 4, and 6.

Creation of the TET-3G LMO1 and TET-3G MYCN Plasmids

The intention for the modification of the AAVS1 locus was to have a heterogeneous integration of LMO1 and MYCN to chromosome 19. To accomplish this task, we created the LMO1 construct controlled by the TET-ON system and the MYCN construct controlled by the TET-ON system.

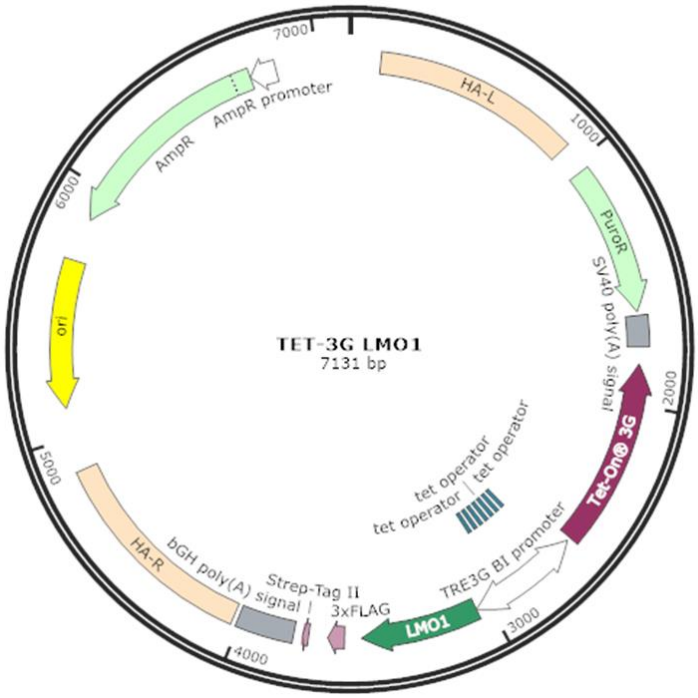

Figure 5. TET-3G LMO1 Plasmid.
The LMO1 gene is regulated by the Tetracycline inducible system and flanked by the HA-L and HA-R homologous arms specific to the AAVS1 locus on chromosome 19.

Figure 6. TET-3G MYCN Plasmid.
The MYCN gene is regulated by the Tetracycline inducible system and flanked by the HA-L and HA-R homologous arms specific to the AAVS1 locus on chromosome 19.

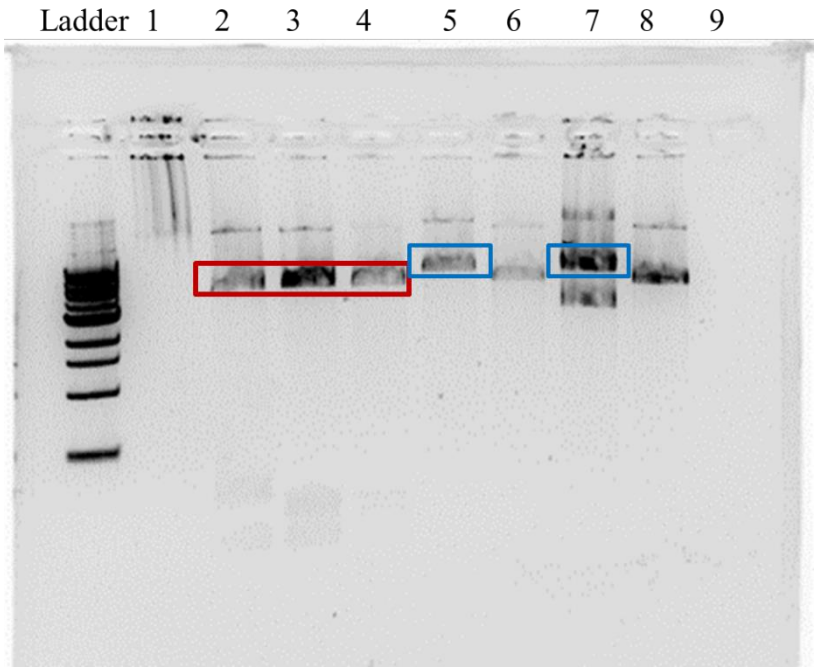

Figure 7. Agarose Gel of TET-3G LMO1 and TET-3G MYCN Constructs. The TET-3G LMO1 is in lanes 1-4 the product for lanes 2-4 is approximately 7.1 kb. The TET-3G MYCN is in lanes5-8 and lanes 5 and 7 are approximately 8kb which correspond with expected product sizes.

Integration of TET-3G LMO1 into H1 hESC

Once the constructs were formed and isolated from bacterial cultures, it was critical to validate the MYCN and LMO1 sequences before H1 hESC nucleofection. The MYCN construct revealed a 24 base pair deletion at the 494-nucleotide position inside the MYCN coding region. The MYCN donor plasmid was sequenced, which reveal the same 24 base pair deletion. The LMO1 construct contained a single nucleotide polymorphism that resulted in a silent mutation that did not alter the LMO1 protein. Based on the sequence analysis, only the TET-3G LMO1 was nucleofected into the H1 hESC.

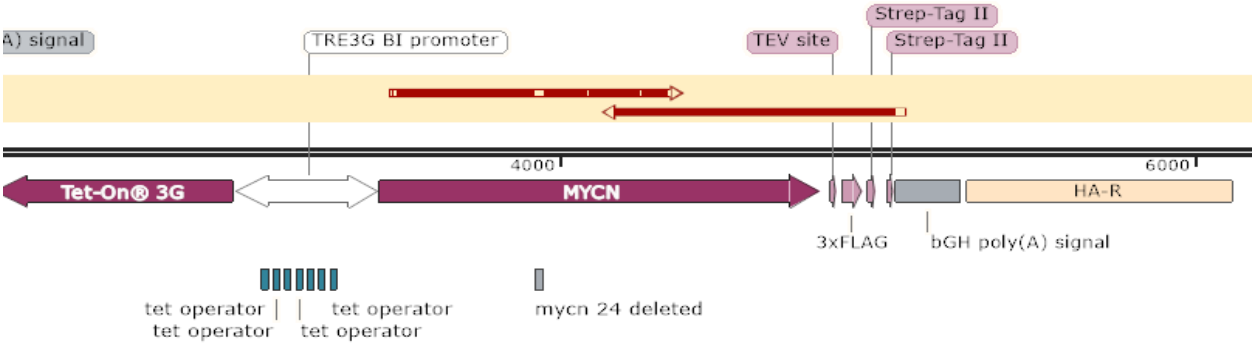

Figure 8. TET-3G MYCN Sequence Alignment.
The TET-3G MYCN has a 24 base pair deletion in the gene which was characterized from sequencing and Snap Gene alignment.

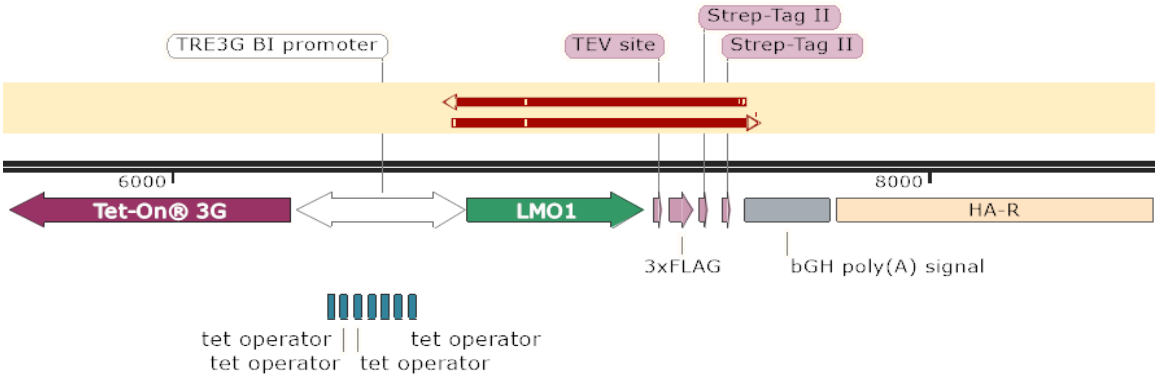

Figure 9. TET-3G LMO1 Sequence Alignment.
The TET-3G LMO1 construct contains a single nucleotide polymorphism that results in a silent mutation.

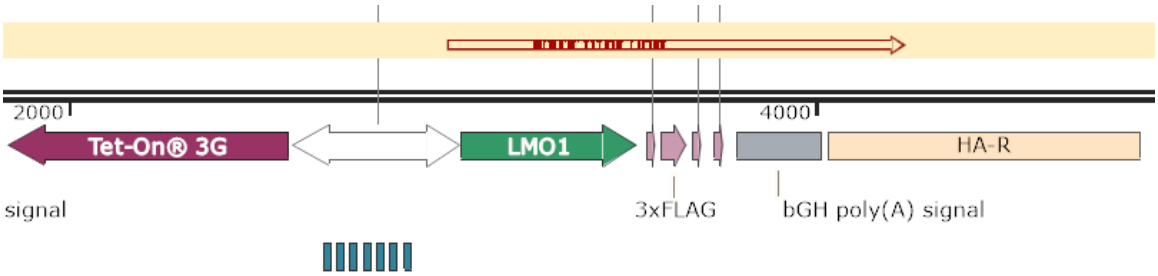

Figure 10. TET-3G LMO1 H1 hESC Sequence Alignment.
The alignment displays a fragmented sequence of the LMO1 coding gene suggesting a small subset of the construct was integrated into the H1 hESC.

CHAPTER FOUR

DISCUSSION AND CONCLUSION

Obstacles and Limitations

The project, in principle, is straightforward, but the development of the cell line required multiple design modifications within a narrow time constraint. The development of the LMO1 and MYCN constructs occurred quickly in the project timeline, but of course, the MYCN mutation was identified once the construct was isolated from bacterial cultures and sequenced. The MYCN repair was complicated as the gene is 66% GC rich, and the region of the 24-base pair deletion contains 92% GC content. These GC dense areas inhibited our ability to modify the region with PCR as temperatures required for annealing were equal to or higher than the polymerase activation temperature. Several piece-wise PCR strategies were undertaken, but repair of the MYCN remained unsuccessful. An alternative strategy considered was using a vector building company to synthesis the MYCN gene; however, due to the GC content and size of our gene, companies were unable to synthesize the gene. To address the GC content and build a synthetic gene, I went through the MYCN gene and created synthetic sequences that replaced cystines and guanines with thymine and adenine but did not alter the protein sequence. This strategy proved to be expensive and outside of the budgetary considerations of the project.

There was a necessity for the constructs have a fluorescent tag to permit screening and selection in the H1 hESC. The MYCN construct never proceeded to the fluorescent modification stage, but the LMO1 construct was created quickly and without issue. There were two fluorescent models for LMO1, the first utilizing an EGFP gene flanked by two loci of X-over P1 (loxP) sites. This model intended to identify the H1 hESC that contained LMO1 and depending on future experimental parameters; the EGFP could be removed. This construct was never synthesized in several Infusion strategies. The second model strategy integrates the EGFP gene into the Tet-3G LMO1 construct, which would permanently express EGFP in the H1 hESC. The EGFP expression was desirable for both selection as well as future tracing in developmental experiments if the cells were implanted into one of the Garcia-Castro animal models. The integration of the EGFP gene did appear successful in the sequence analysis of the gene. However, the transfection of the TET-3G LMO1 EGFP into HEK-293 cells did not produce a fluorescent signal. This test of the EGFP was conducted with the donor EGFP plasmid the gene was isolated from along with a commercial plasmid, both controls produced clear fluorescent signals. The attempts to develop a TET-3G LMO1 construct with a fluorescent marker were time-consuming and unsuccessful, so I decided to continue the project with just the TET-3G LMO1 construct and screen the LMO1 sequence in less efficient manner relying on statistical probability for integration compared to single-cell isolation.

MYCN Development

The MYCN gene on the TET-3G MYCN construct contained a 24-nucleotide deletion at the 494-528 base pair region. To identify if the mutation was a result of the construct engineering, I sequenced the MYCN donor plasmid. The mutation was contained in the donor and was the source of the mutation. The next question that emerged from the sequence analysis was, did the 24-base pair deletion corresponds to an isoform that has been characterized in cancer formation, particularly neuroblastoma. The mutated sequence was uploaded to the NCBI Basic Local Alignment Search Tool (BLAST) to examine the protein characteristics. The MYCN gene contained in the MYCN donor plasmid mapped onto the human MYCN gene but with a 96.99% identity match signifying this mutation has not been characterized previously and could not be integrated into our H1 hESC model in this form. The MYCN construct underwent many attempts to repair the gene using several subcloning strategies. Despite my best efforts, the MYCN gene contains the 24-base pair deletion in both the donor and the TET-3G MYCN plasmids.

LMO1 Development

The isolation of the LMO1 gene was straightforward as I was able to extract it from the neural crest cell cDNA library maintained in the Garcia-Castro lab. Sequencing of the LMO1 gene and analysis with NCBI BLASTX revealed that the protein was an identical match to the human gene. Once the

TET-3G LMO1 plasmid was a development, I repeated the same analysis, and the results were the same, so we set aside a sample of the bacterial stock for long-term storage and proceeded with the H1 hESC nucleofection with the TET-3G LMO1 construct. I maintained the H1 hESC for about a week to permit the nonintegrated plasmid to deteriorate so that analysis would only show sequence analysis from integrated LMO1. The sequence analysis revealed a fragmented sequence of the LMO1 gene along with the flanking sequence of the homologous arms of the TET-3G LMO1 plasmid. However, given that the sequence of the LMO1 gene was fragmented and weaker than the signal obtained from the homologous arms sequence suggest the integration occurred in a small subset of the ESCs, and therefore the cell population is a mixed colony. The establishment of the H1 hESC with the LMO1 cell line is essential for the development of our human NB model as LMO1 has been characterized as a significant oncogene in zebrafish and several GWAS in the United States, Europe, and China.

Conclusion

The development of the TET-3G LMO1 H1 hESC is one component of the human model to understand the role of LMO1 and MYCN in neuroblastoma formation. Like with all scientific research, projects are never truly finished, and there are some immediate experiments I would continue if time permitted. The TET-3G LMO1 H1 ESC must undergo further colony screening to obtain a pure population of stem cells that can be expanded and used in the

development of the LMO1 plus MYCN inducible cell line. Once the LMO1 line is stable, the next step will be to integrate the MYCN gene. Recently, there have been several plasmids containing human MYCN cDNA that has been donated to the company addgene. It would prove beneficial to locate the researchers that developed these plasmids and inquire about their function and gene composition; one of these plasmids may serve as the MYCN gene donor for our experiment. Once the cell line is established, the next component will be to express the LMO1 and MYCN proteins with doxycycline treatments. It is important to mention that before purchasing the TET-3G plasmid, I conducted toxicity tests on H1 hESC with the doxycycline concentrations ranging from 0.25- 2 mg/ml over five days and observed no changes in morphology or impediment to survival. Following the doxycycline treatment to the LMO1 plus MYCN cell line and understanding the parameters needed to maintain H1 hESC morphology, the cells can undergo neural crest cell induction, in which the Garcia-Castro laboratory has an efficient and proven protocol. My role in the project was the development of the H1 ESC cell line, and given the parameters and obstacles we encountered, the members of the Garcia-Castro lab and I believe the development of the H1 hESC LMO1 line is a solid starting point for the continuation of the human neuroblastoma model.

CHAPTER FIVE

METHODS AND MATERIALS

Plasmid Linearization and DNA Purification

PCR linearized the AAVS1 Puro Tet3G 3xFLAG Twin Strep (TET-3G) plasmid with primers AAVS1 TET ON VEC forward and AAVS1 TET ON VEC reverse (Table 1).

1. The PCR was conducted in a SimpliAmp™ Thermal Cycler, using Phusion™ High-Fidelity polymerase under reaction specific cycle conditions (see Table 1).

2. The PCR product ran on a 1% agarose gel mixed with GelRed® Nucleic Acid Gel Stain and visualized in a Bio-Rad Gel Doc™ XR+ Gel Documentation System.
3. The PCR fragment was purified from the gel using the Zymoclean Gel DNA Recovery Kit.

The PCR equipment and DNA purification process for LMO1, MYCN, and EGFP are identical to methods used in TET-3G purification. The only variations are the templates and specific PCR conditions are in Table 1.

Cycling Conditions

One-time Initial denaturation: 95^{O} C for 1 minute

35 cycles: Denature 95^{O} C for 20 seconds
Annealing varied temperature for 10 seconds
Extension 72^{O}C for varied times

Plasmid/ template	Forward Primer	Reverse Primer	Annealing Temp & Extension Time	Purpose
TET-3G	VEC TET ON	AAVS1 TET ON	64^{O} C:10 sec	Infusion
LMO1 cDNA	hLMO1 TET	hLMO1 TET	66^{O} C:10 sec	Infusion
pCDNA3-HA-human W-MYCN	hMYCN TET	hMYCN TET	58^{O} C: 15 sec	Infusion
AAVS1 EGFP donor	CMV EGFP	CMV EGFP	69^{O} C: 25 sec	Infusion

Table 1. PCR Reactions.

Cloning of LMO1 and MYCN into the TET-3G Plasmid

1. The Vector and inserts were ligated using the Takara In-Fusion® cloning kit. The reaction formulations were performed with the Takara In-Fusion® Molar Ratio Calculator tool.
2. The 10 ul cloning mixture was incubated for 15 minutes at 50^{O} C.
3. Following the ligation reaction, 2.5 ul of the TET-3G LMO1 and TET-3G MYCN were added to separate 50 ul of Stellar Super Competent cells, placed on ice for 30 minutes, and proceeded by 45 seconds of heat shock at 42^{O} C.

4. 500ul of 37^{O} C SOC media was added to the transformation reaction and incubated at 37^{O} C for 1 hour on the shaker.
5. The cells were plated on LB ampicillin agar plates and grown for 14 hours at 37^{O} C. Several bacterial colonies from both plasmids were picked and expanded in 2 ml of LB media containing ampicillin for 12-16 hours.
6. A 600 ul sample taken from each 2 ml culture, and the DNA was extracted using a ZymoPURE™ Plasmid Miniprep Kit.
7. Retrogen Inc sequenced the TET-3G LMO1 and TET-3G MYCN plasmids.
8. Based on sequence analysis, 10ul of the TET-3G LMO1 culture was added to 90 ml of LB liquid media containing 90 ul of ampicillin and was grown for 12 hours at 37^{O} C on a shaker.
9. The TET-3G LMO1 DNA was collected with the ZymoPURE™ Plasmid Midiprep Kit.

Creating the TET-3G LMO1 EGFP Plasmid

The TET-3G LMO1 plasmid was linearized by restriction digestion using the enzymes HPA1 and NSI1, incubated at 37^{O} C for 12 hours. The TET-3G LMO1 linear plasmid and EGFP fragment were ligated, verified, and expanded following the methods used in the TET 3G LMO1 plasmid development (shown above).

H1 hESC Nucleofection and Colony Selection

1. Human ESCs were cultured in mTSeR medium with Rho Kinase (ROCK)-inhibitor (10uM, Tocris) for 24 hours before electroporation.

2. Cells were washed three times by Ca/Mg-Free PBS, digested by Accutase (Stem Cell Tech) for 5 minutes, and harvested in mTSeR medium with 10uM ROCK-inhibitor.
3. Cells were dispersed into single cells and counted. Cells at 1.4-1.6x106 density are aliquoted into a 15ml conical tube for each nucleofection.
4. Cells were spun down at 90 x g for 3min at RT.
5. Cells were gently resuspended in 100ul of P3 Nucleofection Buffer (Lonza) containing a combination of plasmids up to 10% of the total volume (10ul max.). 15µg Cas9 plasmid, 15µg each sgRNA plasmid for wild-type Cas9, and 30µg TET-3G LMO1 were used for nucleofection—the ratio of 1:1:2 (cas9: sgRNA: donor plasmid should always be maintained).
6. The cells in P3 buffer +TET-3G LMO1 plasmids were nucleofected using the 4D-Nucleofector System (Lonza) using the CN-137 setting in single 100ul-cuvettes (Lonza).
7. Removed the cuvette and let the cells stand in the cuvette for 2-3mins in the hood after 2-3mins added 500ul of warm mTSeR (with Ri).
8. Plate the cell in the Matrigel wells of a 6-well plate.
9. After 3-4 days, colonies were picked from single cells to screen for clones.

APPENDIX A

AAVS1 INTERGRATION SITE

The creation of the TET-3G LMO1 H1 hESC line was established with the integration of the TET-ON and LMO1 DNA with the CRISPR Cas 9 gene-editing system. The homologs arm on the TET-3G LMO1 have sequence specificity to the AAVS1 integration site on chromosome 19.

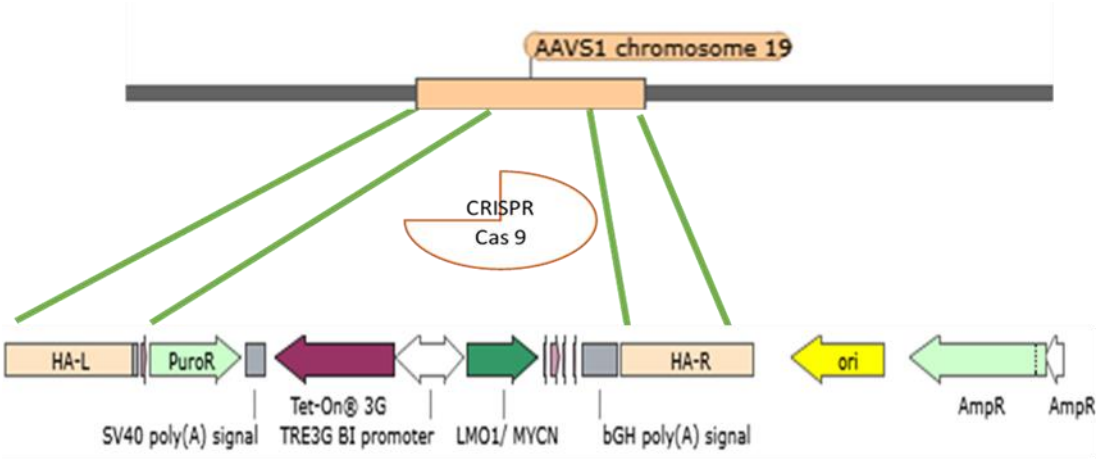

AAVS1 Locus.
Modified by CRISPR Cas 9 homologous directed repair with the AAVS1 arms of the plasmid. The model represents a stand-in position for either the LMO1 or MYCN gene. However, the actual construct would contain only one of the genes, and heterozygous integration is the correct alteration of the H1 ESC genome.

AAVS1 (adeno-associated virus integration site)

GAATTCCTAACTGCCCCGGGGCAGTCTGCTATTCATCCCCTTTACGCGGTG
CTACACACACTTGCTAGTATGCCGTGGGGACCCCTCCGGCCTGTAGACTCC
ATTTCCCAGCATTCCCCGGAGGAGGCCCTCATCTGGCGATTTCCACTGGGG
GCCTCGGAGCTGCGGACTTCCCAGTGTGCATCGGGGCACAGCGACTCCTG
GAAGTGGCCACTTCTGCTAATGGACTCCATTTCCCAGGCTCCCGCTACCTG
CCCAGCACACCCTGGGGCATCCGTGACGTCAGCAAGCCGGGCGGGGACC
GGAGATCCTTGGGGCGGTGGGGGGCCAGCGGCAGTTCCCAGGCGGCCCC
CGGGGCGGGCGGGCGGGCGGGTGGTGGCGGCGGTTGGGGCTCCGGGCG
CGTCGCTCGCTCGCTCGCTGGGCGGGCGGGCGGTGCGATGTCCGGAGAG
GATGGCCGGCGGCTGGCCCGGGGGCGGCGGCGCGGCTGCCCGGGAGCG
GCGACGGGAGCAGCTGCGGCAGTGGGGCGCGGGCGGGCGCCGAGCCTG
GCCCCGGAGAGCGCCGCGCCCGCACCGTCCGCTTCGAGCGCGCCGCCGA
GTTCCTGGCGGCCTGTGCGGGCGGCGACCTGGACGAGGCGCGTCTGATG
CTGCGCGCCGCCGACCCTGGCCCCGGCGCCGGAGCTCGACCCCGCCGGC
CGCCGCCCGCCCGCGCCGTGCTGGACTCCACCAACGCCGACGGTATCAGC
GCCCTGCACCAGGTCAGCGCCCCCCGCGGCGTCTCCCGGGGCCAGGTCC
ACCCTCTGCGCCACCTGGGGCATCCTCCTTCCCCGTTGCCAGTCTCGATCC
GCCCCGTCGTTACTGGCCCTGGGTTTNCACCCTATGCTGACACCCCGTTCC
AGTCCCCTTACCATTCCCTTCGACCACCCCACTTCCGAATTGGAGCGCTTCA
ACTGGCTGGGCTAGCACTCTGTGTGACACTCTGAAGCTCTACATTCCCTTC
GACCTACTCTCTTCGATTGGAGTCGCTTTAACTGGCCCTGGCTTTGGCAGC
CTGTGCTGACCCATCGAGTCCTCCTTACCATCCCTCCCTCGACTTCCCCTCT
TCCGATGTTGAGCCCCTCCAGCCGGTCCTGGACTTTGTCTCCTTCCCTGCC
CTGCCCTCTCCTGAACCTGAGCCAGCTCCCATAGCTCAGGTCTGGTCTATC
TGCCTGGCCCTGGCCATTGTCACTTTGCGCTGCCCTCCTCTCGCCCCCGAG
TGCCCTTGCTGTGCCGCCGGAACTCTGCCCTCTAACGCTGCCGTGCCGTCT
CTCTCCTGAGTCCGGACCACTTTGAGCTCTACTGGCTTCTGCGCGCCTCTG
GCCCACTGTTTCCCCTTCCCAGGCAGGTCCTGCTTTCTCTGACCAGCATTCT
CTCCCCTGGGCCTGTGCCGCTTTCTGTCTGCAGCTTGTGGCCTGGGTCACC
TCTACGGCTGGCCCAAGATCCTTCCCTGCCGCCTCCTTCAGGTTCCGTCTT
CCTCCACTCCCTCTTCCCCTTGCTCTCTGCTGTGTTGCTGCCCAAGGATGCT
CTTTCCGGAGCACTTCCTTCTCGGCGCTGCACCACGTGATGTCCTCTGAGC
GGATCCTCCCCGTGTCTGGGTCCTCTCCGGGCATCTCTCCTCCCTCACCCA
ACCCCATGCCGTGTTCACTCGCTGGGTTCCCTTTTCCTTCTCCTTCTGGGGC
CTGTGCCATCTCTCGTTTCTTAGGATGGCCTTCTCCGACGGATGTCTCCCTT
GCGTCCCGCCTCCCCTTCTTGTAGGCCTGCATCATCACCGTTTTTCTGGACA
ACCCCAAAGTACCCCGTCTCCCTGGCTTAGCACCTCTCCATCCTCTTGCTTT
CTTTGCCTGGACACCCCGTTCTCCTGTGGATTCGGGTCACCTCTCACTCCTT
TCATTTGGGCAGCTCCCCTACCCCCCTTACCTCTCTAGTCTGTGCTAGCTCT
TCCAGCCCCCTGTCATGGCATCTTCCAGGGGTCCGAGAGCTCAGCTAGTCT
TCTTCCTCCAACCCGGGCCCTATGTCCACTTCAGGACAGCATGTTTGCTGC

CTCCAGGGATCCTGTGTCCCCGAGCTGGGACCACCTTATATTCCCAGGGCC
GGTTAATGTGGCTCTGGTTCTGGGTACTTTTATCTGTCCCCTCCACCCCACA
GTGGGGCCACTAGGGACAGGATTGGTGACAGAAAAGCCCCCATCCTTAGG
CCTCCTCCTTCCTAGTCTCCTGATATTCGTCTAACCCCCACCTCCTGTTAGG
CAGATTCCTTATCTGGTGACACACCCCCATTTCCTGGAGCCATCTCTCTCCT
TGCCAGAACCTCTAAGGTTTGCTTACGATGGAGCCAGAGAGGATCCTGGGA
GGGAGACTTGGCAGGGGGTGGGAGGGAAGGGGGGGATGCGTGACCTGCC
CGGTTCTCAGTGGCCACCCTGCGCTACCCTCTCCCAGAACCTGAGCTGCTC
TGACGCGGCTGTCTGGTGCGTTTCACTGATCCTGGTGCTGCAGCTTCCTTA
CACTTCCCAAGAGGAGAAGCAGTTTGGAAAAACAAAATCAGAATAAGTTGGT
CCTGAGTTCTAACTTTGGCTCTTCACCTTTCTAGNCCCCAATTTATATTGTTC
CTCCGTGCGTCAGTTTTACCTGTGAGATAAGGCCAGTAGCCACCCCCGTCC
TGGCAGGGCTGTGGTGAGGAGGGGGGTGTCCGTGTGGAAAACTCCCTTTG
TGAGAATGGTGCGTCCTAGGTGTTCACCAGGTCGTGGCCGCCTCTACTCCC
TTTCTCTTTCTCCATCCATCCTTCTTTCCTTAAAGAGCCCCCAGTGCTATCTG
GACATATTCCTCCGCCCAGAGCAGGGTCCGCTTCCCTAAGGCCCTGCTCTG
GGCTTCTGGGTTTGAGTCCTTGCAAGCCCAGGAGAGCGCTAGCTTCCCTGT
CCCCCTTCCTCGTCCACCATCTCATGCCCTGGCTCTCCTGCCCCTTCCTACA
GGGGTTCCTGGCTCTGCTCTTCAGACTGAGCCCCGTTCCCCTGCATCCCCG
TTCCCCTGCATCCCCCTTCCCCTGCATCCCCCAGAGCCCCAGGCCACCTAC
TTGGCCTGGAACCCCACGAGAGGCCACCCCAGCCCTGTCTACCAGGCTGA
CCTTTTGGGTGATTCTCCTCCAACTGTGGGGTGACTGCTTGGGCAAACTCA
CTCTTCGGGGTATCCCAGGAGGCCTGGAGCATTGGGGTGGGCTGGGGTTC
AGAGAGGAGGGATTCCCTCCAGGTTACGTGGCCAAGAAGCAGGGGAGCTG
GGTTTGGGTCAGGCTGGGTGTGGGGTGACCAGCTTATGCTGTTTGCCCAG
GACAGCCTAGTTTTAGCGCTGAAACCCTCAGTCCTAGGAAAACAGGGATGG
TTGGTCACTGTCTCTGGGTGACTCTTGATTCCCGGCCAGTTTCTCCACCTGG
GGCTGTGTTTCTCGTCCTGCATCCTTCTCCAGGCAGGTCCCCAAGCATCGC
CCCCCTGGCTGTTCCCAAGTTCTTAGGTACCCCACGTGGGTTTATGAACCA
CTTGGTGAGGCTGGTACCCTGCCCCCATTCCTGCACCCCAATTGCCTTAGT
GGCTAGGGGGTTGGGGGCTAGAGTAGGAGGGGCTGGAGCCAGGATTCTTA
GGGCTGAACAGAGCCGAGCTGGGGGCCTGGGCTCCTGGGTTTGAGAGAG
GAGGGGCTGGGGCCTGGACTCCTGGGTCCGAGGGAGGAGGGGCTGGGG
CCTGGACTCCTGGGTCTGAGGGTGGAGGGACTGGGGGCCTGGACTCCTGG
GTCCGAGGGAGGAGGGGCTGGGGCCTGGACTCGTGGGTCTGAGGGAGGA
GGGGTCGGGGGCCTGGACTTCTGGGTCTTAGGGAGGCGGGGCTGGGCCT
GGACCCCTGGGTCTGAATGGGGAGAGGCTGGGGGCCTGGACTCCTTCATC
TGAGGGCGGAAGGGCTGGGGCCTGGCCTCCTGGGTTGAATGGGGAGGGG
TTGGGCCTGGACTCTGGAGTCCCTGGTGCCCAGGCCTCAGGCATCTTTCAC
AGGGATGCCTGTAC

AAVS1 Homologous Arms Sequence.
The blue font corresponds to the homologous left arm of the TET-3G LMO1, and the right font corresponds to the TET-3G LMO1 homologous right arm.

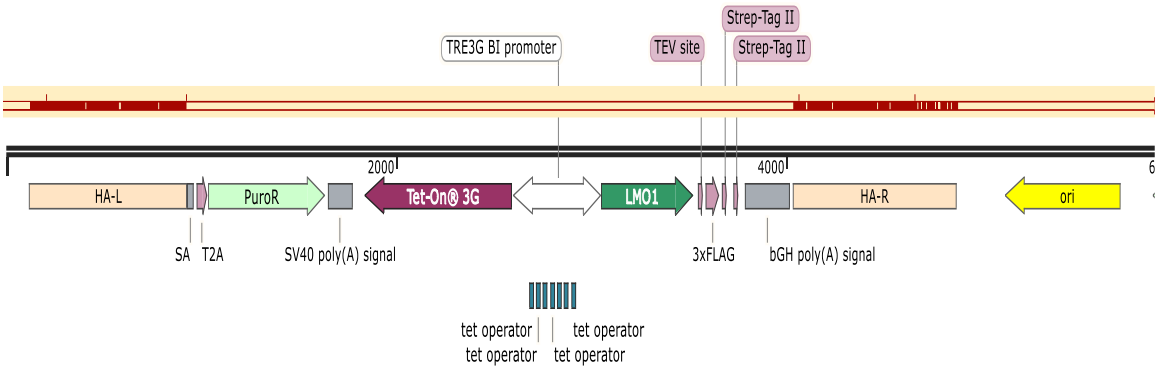

TET-3G LMO1 Homologous Arms Alignment.
The alignment of the AAVS1 integration site with the TET-3G LMO1 plasmid demonstrating the homology that permits integration into the H1 hESC.

REFERENCES

Althoff, K., Beckers, A., Bell, E., Nortmeyer, M., Thor, T., Sprüssel, A., Lindner, S., De Preter, K., Florin, A., Heukamp, L. C., Klein-Hitpass, L., Astrahantseff, K., Kumps, C., Speleman, F., Eggert, A., Westermann, F., Schramm, A., & Schulte, J. H. (2015). A Cre-conditional MYCN-driven neuroblastoma mouse model as an improved tool for preclinical studies. Oncogene, 34(26), 3357–3368. https://doi.org/10.1038/onc.2014.269

Bach, I. (2000). The LIM domain: regulation by association. Mechanisms of development, 91(1-2), 5–17. https://doi.org/10.1016/s0925-4773(99)00314-7

Beltran, H., Rickman, D. S., Park, K., Chae, S. S., Sboner, A., MacDonald, T. Y., Wang, Y., Sheikh, K. L., Terry, S., Tagawa, S. T., Dhir, R., Nelson, J. B., de la Taille, A., Allory, Y., Gerstein, M. B., Perner, S., Pienta, K. J., Chinnaiyan, A. M., Wang, Y., Collins, C. Molecular characterization of neuroendocrine prostate cancer and identification of new drug targets. *Cancer discovery*, *1*(6), 487–495. https://doi.org/10.1158/2159-8290.CD-11-0130

Bosse, K. R., & Maris, J. M. (2016). Advances in the translational genomics of neuroblastoma: From improving risk stratification and revealing novel biology to identifying actionable genomic alterations. Cancer, 122(1), 20–33. https://doi.org/10.1002/cncr.29706

Brodeur, G. M., Seeger, R. C., Schwab, M., Varmus, H. E., & Bishop, J. M. (1984). Amplification of N-myc in untreated human neuroblastomas correlates with advanced disease stage. *Science (New York, N.Y.)*, *224*(4653), 1121–1124. https://doi.org/10.1126/science.6719137

Brodeur G. M. (2003). Neuroblastoma: biological insights into a clinical enigma. Nature reviews. Cancer, 3(3), 203–216. https://doi.org/10.1038/nrc1014

Cheung, N. K., & Dyer, M. A. (2013). Neuroblastoma: developmental biology, cancer genomics and immunotherapy. Nature reviews. Cancer, 13(6), 397–411. https://doi.org/10.1038/nrc3526

Colon, N. C., & Chung, D. H. (2011). Neuroblastoma. Advances in pediatrics, 58(1), 297–311. https://doi.org/10.1016/j.yapd.2011.03.011

Dang C. V. (2012). MYC on the path to cancer. Cell, 149(1), 22–35. https://doi.org/10.1016/j.cell.2012.03.003

Das, A. T., Tenenbaum, L., & Berkhout, B. (2016). Tet-On Systems For Doxycycline-inducible Gene Expression. Current gene therapy, 16(3), 156–167. https://doi.org/10.2174/1566523216666160524144041

Dupin E, Creuzet S, Le Douarin, NM. The Contribution of the Neural Crest to the Vertebrate Body. In: Madame Curie Bioscience Database [Internet]. Austin (TX): Landes Bioscience; 2000-2013. Available from: https://www.ncbi.nlm.nih.gov/books/NBK6098/

Gilbert SF. Developmental Biology. 6th edition. Sunderland (MA): Sinauer Associates; 2000. The Neural Crest. Available from: https://www.ncbi.nlm.nih.gov/books/NBK10065/

Huang, M., & Weiss, W. A. (2013). Neuroblastoma and MYCN. Cold Spring Harbor perspectives in medicine, 3(10), a014415. https://doi.org/10.1101/cshperspect.a014415

Huber, K. (2015). Segregation of neuronal and neuroendocrine differentiation in the sympathoadrenal lineage. Cell and tissue research, 359(1), 333–341. https://doi.org/10.1007/s00441-014-1947-0
Janoueix-Lerosey, I., Lequin, D., Brugières, L. et al. Somatic and germline activating mutations of the ALK kinase receptor in neuroblastoma. Nature 455, 967–970 (2008). https://doi.org/10.1038/nature07398

Kawauchi D, Robinson G, Uziel T, et al. A mouse model of the most aggressive subgroup of human medulloblastoma. Cancer Cell. 2012;21(2):168-180. doi:10.1016/j.ccr.2011.12.023

Kim J, Lo L, Dormand E, Anderson DJ . SOX10 maintains multipotency and inhibits neuronal differentiation of neural crest stem cells. Neuron 2003; 38: 17–31.

Kim, S., & Chung, D. H. (2006). Pediatric solid malignancies: neuroblastoma and Wilms' tumor. The Surgical clinics of North America, 86(2), 469–xi. https://doi.org/10.1016/j.suc.2005.12.008

Knoepfler, P. S., Cheng, P. F., & Eisenman, R. N. (2002). N-myc is essential during neurogenesis for the rapid expansion of progenitor cell populations and the inhibition of neuronal differentiation. Genes & development, 16(20), 2699–2712. https://doi.org/10.1101/gad.1021202

Knudson, A. G., Jr, & Strong, L. C. (1972). Mutation and cancer: neuroblastoma and pheochromocytoma. American journal of human genetics, 24(5), 514–532.
Kushner B. H. (2004). Neuroblastoma: a disease requiring a multitude of imaging

studies. Journal of nuclear medicine: official publication, Society of Nuclear Medicine, 45(7), 1172–1188.

Maris J. M. (2010). Recent advances in neuroblastoma. The New England journal of medicine, 362(23), 2202–2211. https://doi.org/10.1056/NEJMra0804577

Matthay, K. K., George, R. E., & Yu, A. L. (2012). Promising therapeutic targets in neuroblastoma. Clinical cancer research: an official journal of the American Association for Cancer Research, 18(10), 2740–2753. https://doi.org/10.1158/1078-0432.CCR-11-1939

Matthews, J. M., Lester, K., Joseph, S., & Curtis, D. J. (2013). LIM-domain-only proteins in cancer. Nature reviews. Cancer, 13(2), 111–122. https://doi.org/10.1038/nrc3418

Modak, S., & Cheung, N. K. (2010). Neuroblastoma: Therapeutic strategies for a clinical enigma. Cancer treatment reviews, 36(4), 307–317. https://doi.org/10.1016/j.ctrv.2010.02.006

Mossé, Y. P., Laudenslager, M., Longo, L., Cole, K. A., Wood, A., Attiyeh, E. F., Laquaglia, M. J., Sennett, R., Lynch, J. E., Perri, P., Laureys, G., Speleman, F., Kim, C., Hou, C., Hakonarson, H., Torkamani, A., Schork, N. J., Brodeur, G. M., Tonini, G. P., Rappaport, E., … Maris, J. M. (2008). Identification of ALK as a major familial neuroblastoma predisposition gene. Nature, 455(7215), 930–935. https://doi.org/10.1038/nature07261

Mossé, Y. P., Laudenslager, M., Khazi, D., Carlisle, A. J., Winter, C. L., Rappaport, E., & Maris, J. M. (2004). Germline PHOX2B mutation in hereditary neuroblastoma. *American journal of human genetics*, *75*(4), 727–730. https://doi.org/10.1086/424530

Olsen RR, Otero JH, García-López J, et al. MYCN induces neuroblastoma in primary neural crest cells. Oncogene. 2017;36(35):5075-5082. doi:10.1038/onc.2017.128

Pagès, P. M., Dufour, C., Fasola, S., Michon, J., Boutard, P., Gentet, J. C., & Hartmann, O. (2009). Bilateral adrenal neuroblastoma. *Pediatric blood & cancer*, *52*(2), 196–202. https://doi.org/10.1002/pbc.21765

Park, J. R., Eggert, A., & Caron, H. (2010). Neuroblastoma: biology, prognosis, and treatment. Hematology/oncology clinics of North America, 24(1), 65–86. https://doi.org/10.1016/j.hoc.2009.11.011

Prasad, MS, Charney RM, García-Castro, MI. Specification and formation of the neural crest: Perspectives on lineage segregation. Genesis. 2019;57(1):e23276. doi:10.1002/dvg.23276

Pugh, T. J., Morozova, O., Attiyeh, E. F., Asgharzadeh, S., Wei, J. S., Auclair, D., Carter, S. L., Cibulskis, K., Hanna, M., Kiezun, A., Kim, J., Lawrence, M. S., Lichenstein, L.,
McKenna, A., Pedamallu, C. S., Ramos, A. H., Shefler, E., Sivachenko, A., Sougnez, C., Stewart. (2011). The genetic landscape of high-risk neuroblastoma. Nature genetics, 45(3), 279–284. https://doi.org/10.1038/ng.2529

Sadelain, M., Papapetrou, E. P., & Bushman, F. D. (2011). Safe harbours for the integration of new DNA in the human genome. Nature reviews. Cancer, 12(1), 51–58. https://doi.org/10.1038/nrc3179

Schulte, J. H., Lindner, S., Bohrer, A., Maurer, J., De Preter, K., Lefever, S., Heukamp, L., Schulte, S., Molenaar, J., Versteeg, R., Thor, T., Künkele, A., Vandesompele, J., Speleman, F., Schorle, H., Eggert, A., & Schramm, A. (2013). MYCN and ALKF1174L are sufficient to drive neuroblastoma development from neural crest progenitor cells. Oncogene, 32(8), 1059–1065. https://doi.org/10.1038/onc.2012.106

Seeger, R. C., Brodeur, G. M., Sather, H., Dalton, A., Siegel, S. E., Wong, K. Y., & Hammond, D. (1985). Association of multiple copies of the N-myc oncogene with rapid progression of neuroblastomas. The New England journal of medicine, 313(18), 1111–1116. https://doi.org/10.1056/NEJM198510313131802

Simões-Costa, M., & Bronner, M. E. (2015). Establishing neural crest identity: a gene regulatory recipe. Development (Cambridge, England), 142(2), 242–257. https://doi.org/10.1242/dev.105445

Smith, V., & Foster, J. (2018). High-Risk Neuroblastoma Treatment Review. Children (Basel, Switzerland), 5(9), 114. https://doi.org/10.3390/children5090114

Trochet, D., Bourdeaut, F., Janoueix-Lerosey, I., Deville, A., de Pontual, L., Schleiermacher, G., Coze, C., Philip, N., Frébourg, T., Munnich, A., Lyonnet, S., Delattre, O., & Amiel, J. (2004). Germline mutations of the paired-like homeobox 2B (PHOX2B) gene in neuroblastoma. *American journal of human genetics*, *74*(4), 761–764. https://doi.org/10.1086/383253

Vandesompele, J., Baudis, M., De Preter, K., Van Roy, N., Ambros, P., Bown, N., Brinkschmidt, C., Christiansen, H., Combaret, V., Lastowska, M., Nicholson, J., O'Meara, A., Plantaz, D., Stallings, R., Brichard, B., Van den Broecke, C., De Bie, S., De Paepe, A., Laureys, G., & Speleman, F. (2005). Unequivocal delineation of clinicogenetic subgroups and development of a new model for improved outcome prediction in neuroblastoma. Journal of clinical oncology: official journal of the American Society of Clinical Oncology, 23(10), 2280–2299. https://doi.org/10.1200/JCO.2005.06.104

Van Roy, N., De Preter, K., Hoebeeck, J., Van Maerken, T., Pattyn, F., Mestdagh, P., Vermeulen, J., Vandesompele, J., & Speleman, F. (2009). The emerging molecular pathogenesis of neuroblastoma: implications for improved risk assessment and targeted therapy. Genome medicine, 1(7), 74. https://doi.org/10.1186/gm74

Wang K, Diskin SJ, Zhang H, et al. Integrative genomics identifies LMO1 as a neuroblastoma oncogene. Nature. 2011;469(7329):216-220. doi:10.1038/nature09609

Weiss, W. A., Aldape, K., Mohapatra, G., Feuerstein, B. G., & Bishop, J. M. (1997). Targeted expression of MYCN causes neuroblastoma in transgenic mice. The EMBO journal, 16(11), 2985–2995.https://doi.org/10.1093/emboj/16.11.2985

Zhu, S., Zhang, X., Weichert-Leahey, N., Dong, Z., Zhang, C., Lopez, G., Tao, T., He, S., Wood, A. C., Oldridge, D., Ung, C. Y., van Ree, J. H., Khan, A., Salazar, B. M., Lummertz da Rocha, E., Zimmerman, M. W., Guo, F., Cao, H., Hou, X., Weroha, S. J., … Look, A. T. (2017). LMO1 Synergizes with MYCN to Promote Neuroblastoma Initiation and Metastasis. Cancer cell, 32(3), 310–323.e5. https://doi.org/10.1016/j.ccell.2017.08.002